Residual stress in sputtered and evaporated thin films: a ML approach

Tong Su

School of Engineering, Brown University, Providence RI 02912

GitHub repository: https://github.com/tongsu-brown/DATA1030_project.git

1. Introduction

Residual stress is ubiquitous in thin films and can drive delamination/buckling, MEMS deformation, and reliability failures in microelectronic interconnects[1-3]. Stress depends on material, growth conditions, and microstructural evolution, and is commonly interpreted using physical kinetic models and in-situ wafer-curvature measurements[4-6]. In previous work[7], we have developed explicit physical models and mathematical solutions for residual stress evolution in single element metal, binary solid solution and nitrides. But this method is highly constrained by physics mechanisms and assumptions and does not always generalize across a heterogeneous literature-derived database.

Here, we reorganize a curated stress thickness database into a supervised regression problem: predict the film stress at a given thickness using process conditions and basic material descriptors. The goal is to quantify how far a pure data-driven baseline can go on this dataset, identify which predictors matter most, and provide guidance for future hybrid physics-ML modeling. The dataset has 19504 data points and 259 different groups (different materials, lab source and process conditions)[8-40]. There is no previous comparable ML benchmark for this dataset.

2. EDA

For simplicity, only three major EDA interpretations for the thin film stress dataset are given here. Figure 1 gives a basic picture of how the stress-thickness data looks like. The stress-thickness behaves differently for each material and processing conditions. It gets higher with higher positive value (tensile stress) or get smaller with larger negative value (compressive stress). This interpretation shows that the stress-thickness is highly dependent on the different deposition materials and the processing conditions.

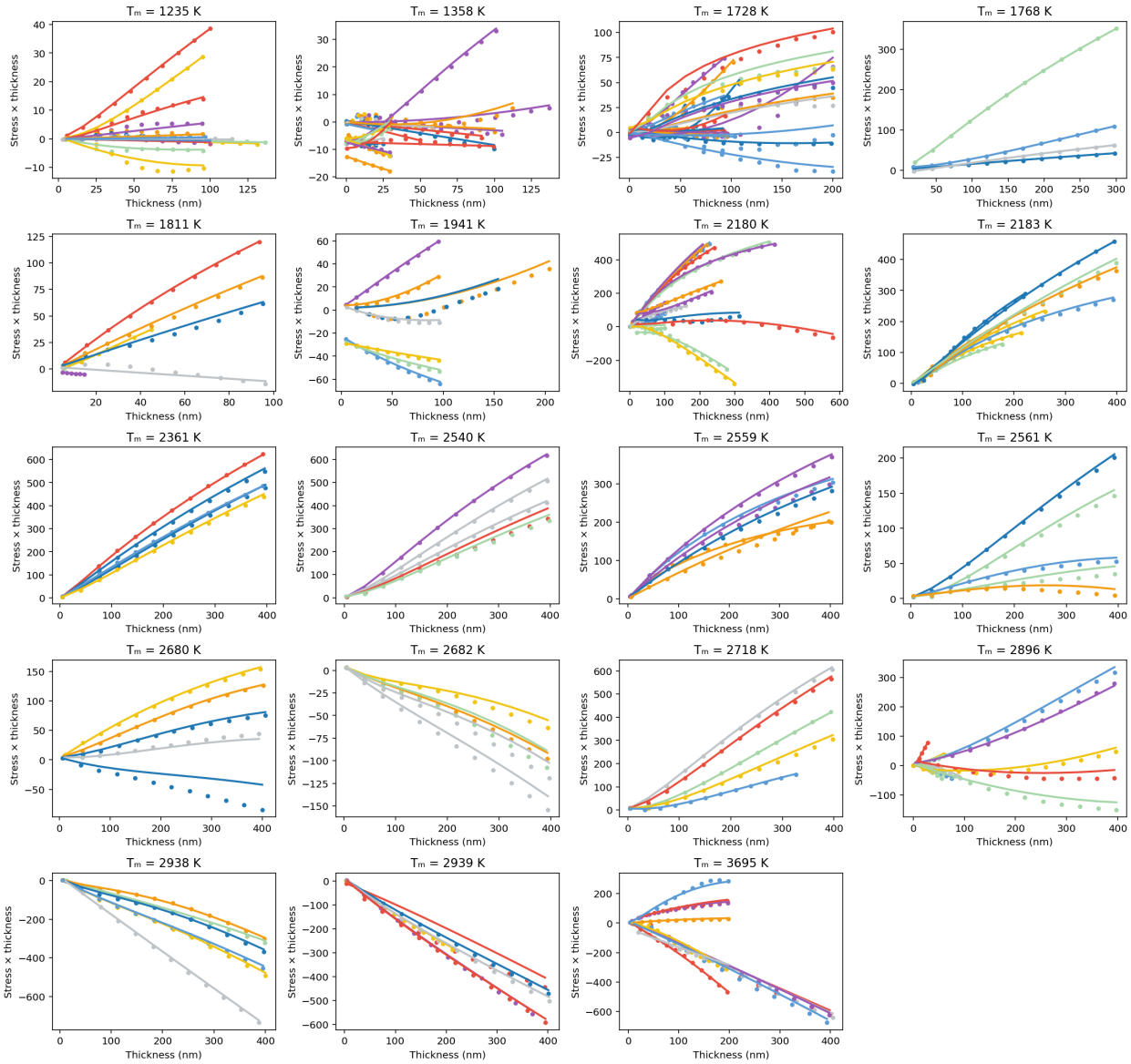

Figure 1, stress thickness raw data (dots) and analytical predictions (solid lines) for 19 different materials.

Figure 2 gives the number of the different crystal structures for the different alloy system. Crystal structure can be A15, BCC, FCC or HCP and alloy system is single element (just one element) or solid solution (two or more elements that can form complete solid solution). It indicates that the crystal structure may have some impact on stress-thickness. But from the stress mechanism speaking, the crystal structure should not affect thin film stress evolution. It can be a good test point in the importance of evaluation to see whether this data pattern can against physics instinct.

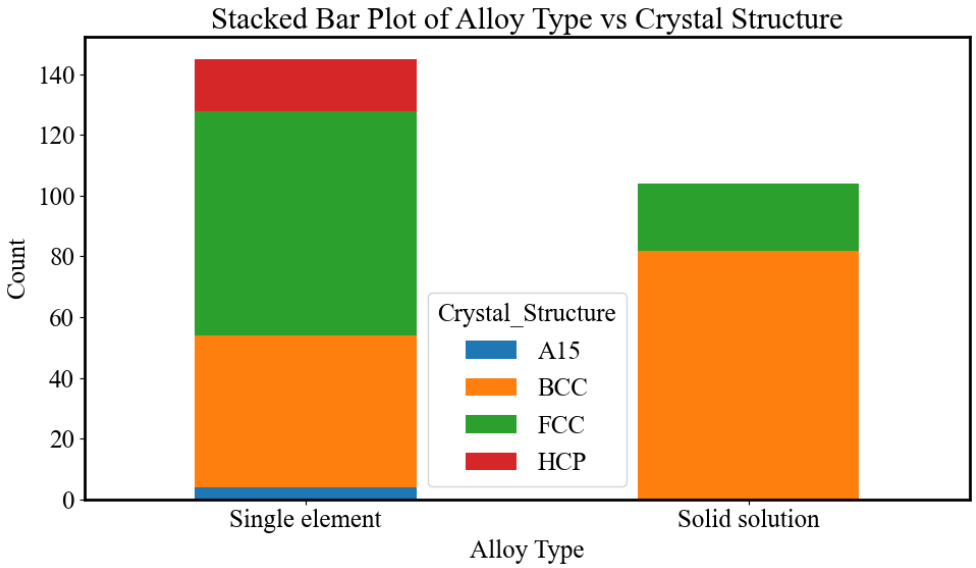

Figure 2, counts of the crystal structure for single element thin film and solid solution

Figure 3 represents the different kinds of substate we can have in the dataset. The most common one is silicon with oxide layer. Some thin films were deposited on the metal layer or ionic layers. Same as the crystal structure, this property should have no impact on the thin film stress. But this parameter is found to be too complex as many datasets come from the intermetallic alloys system, which is not included in the current testing yet. So this feature is excluded from the final model tuning.

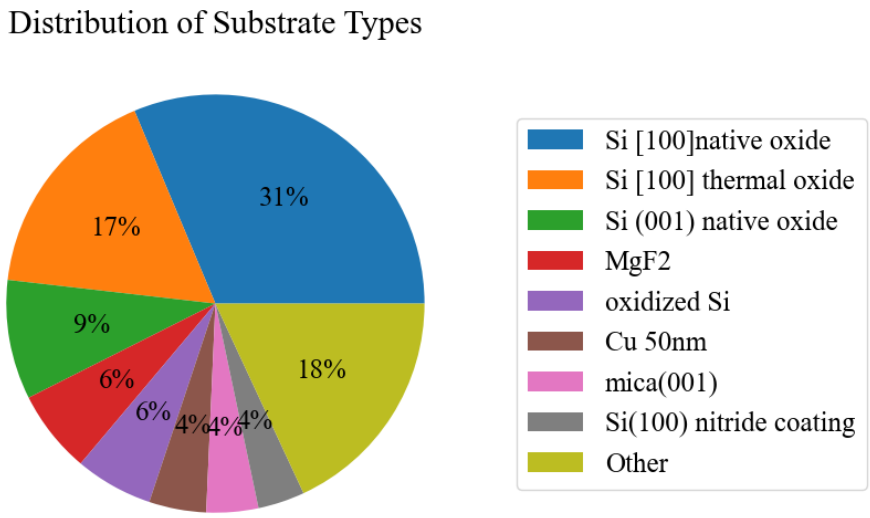

Figure 3, share of the substrate type in the stress thickness database

3. Methods

We treat the task as supervised regression. Each row in data base corresponds to one thickness point on a stress thickness curve. Inputs include numeric features: growth rate R, pressure P, substrate temperature T, thickness, and melting temperature Tm_K; and categorical features: data source (lab/literature), alloy type, and crystal structure.

Splitting strategy: we use nested cross-validation to avoid leakage during hyperparameter tuning. In the outer loop we perform 10 repeated 90/10 GroupShuffleSplit evaluations. Two grouping definitions are compared: (i) grouping by material so the model must generalize to unseen materials; and (ii) grouping by growth rate R to mimic predicting a new process window within materials already seen in training. Inside each outer-train split, a 4-fold K-Fold inner loop selects hyperparameters.

Preprocessing: a single scikit-learn Pipeline is used for all models. Numeric features are standardized (StandardScaler) and categorical features are one-hot encoded (OneHotEncoder with handle_unknown='ignore'). Missing categorical values is treated as a new category.

Models and metrics: we compare five algorithms covered in class: Elastic Net (linear), Random Forest, Gradient Boosting, Support Vector Regression, and K-Nearest Neighbors (non-linear). Dummy Regressor is used as baseline. Hyperparameters and ranges are listed below. RMSE is the primary optimization metric (same units as stress and more sensitive to large errors), and R^2 is reported for interpretability. Uncertainty is summarized as mean ± standard deviation across outer splits (across repeated random seeds for stochastic models).

Hyperparameter grids: Elastic Net (α: 1e−4 -1e3; l1 ratio: 0.1–0.9); Random Forest (max_depth: None or 2–20; max_features: sqrt/log2/None); Gradient Boosting (n_estimators: 200–2000; learning_rate: 1e−3–0.5); SVR (kernel: rbf/linear/poly; C: 0.1–1000); KNN (n_neighbors: 2–7; weights: uniform/distance).

4. Results

Figures 4–8 summarize predictive performance across the different splitting strategies. When the split is grouped by material (Figure 4), all models degrade substantially relative to within-material splits, indicating that generalizing to unseen materials is the hardest setting for this dataset. This outcome suggests that the available material descriptors are not sufficient to fully transfer learned relationships between dissimilar materials. In contrast, grouping by growth rate R (Figure 5) yields noticeably better generalization: the non-linear, tree-based models (Random Forest and Gradient Boosting) outperform linear baselines and achieve lower error with smaller split-to-split variability. Restricting the data to a single data source (Figure 6) further improves performance, supporting the interpretation that cross-dataset shifts contribute non-trivially to error.

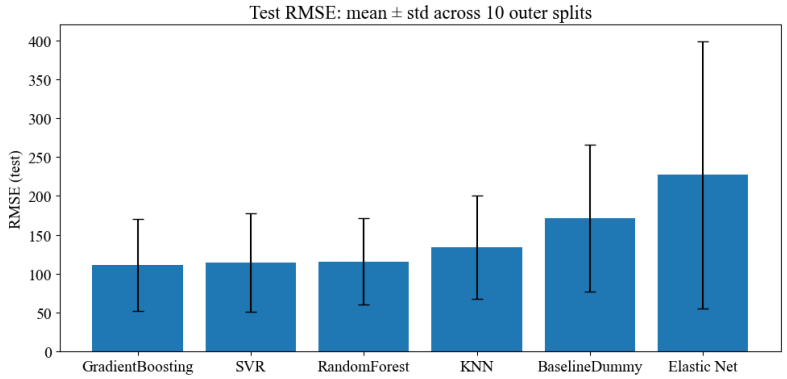

Figure 4, RMSE for different models on data grouping by materials (Tm_K)

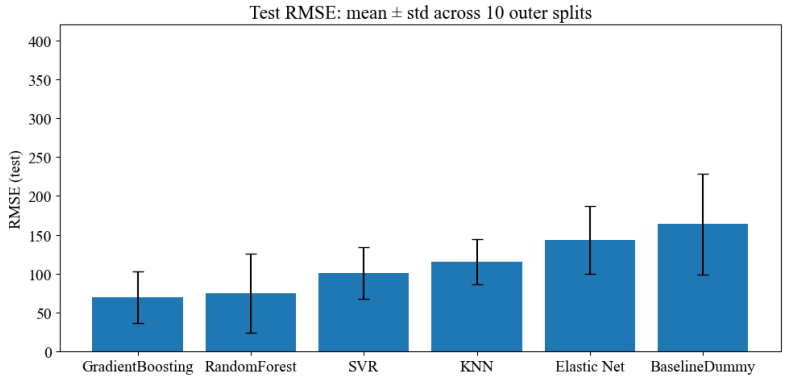

Figure 5, RMSE for different models on data grouping by growth rate R

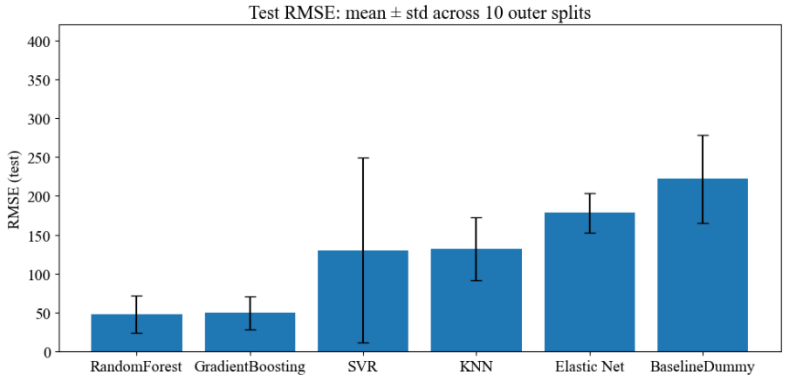

Figure 6, RMSE for different models on data grouping by growth rate R on only one data source

To complement RMSE, Figure 7 reports test-fold and out-of-fold (OOF) R^2. The same model ranking emerges: the tree-based models provide the highest and most consistent R^2 across splits, while linear models tend to underfit. The OOF estimate is particularly informative because it aggregates predictions for every sample made strictly in a held-out split, yielding a fair, non-overlapping estimate of generalization. Figure 8 visualizes OOF predictions against the raw stress–thickness curves. Most predicted curves track the experimental trends well across thickness, with a small number of clear outliers that likely correspond to atypical conditions or under-represented materials.

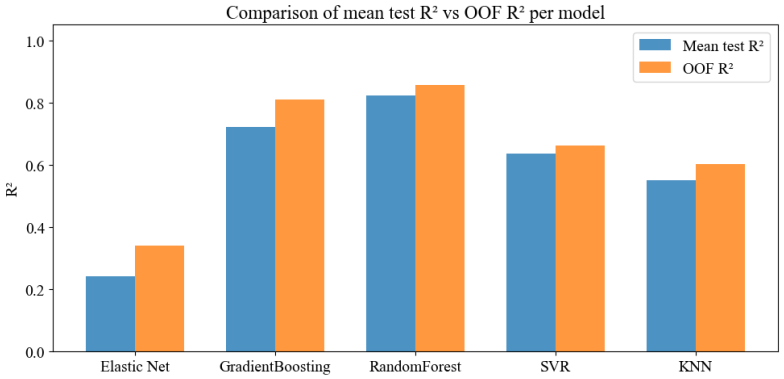

Figure 7, R^2 value of average test fold and OOF for data grouping by growth rate R

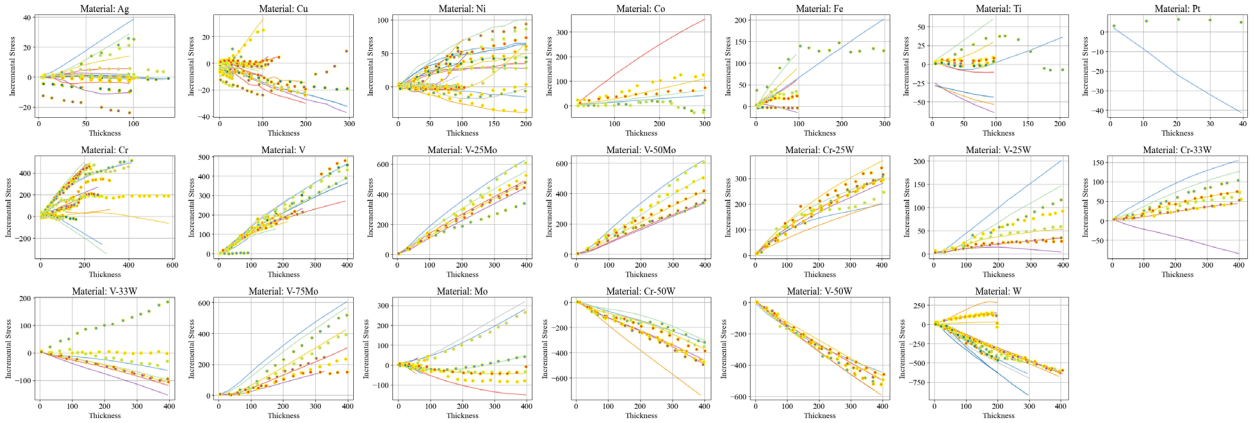

Figure 8, OOF scatter plot for the data grouping by R, the line are raw data from experiments and dots are OOF predictions.

Model interpretability was assessed using three complementary global feature-importance methods for the best-performing Random Forest model (Figure 9a–c): (a) permutation importance, (b) SHAP global importance (mean absolute SHAP value), and (c) the Random Forest built-in impurity-based importance. All three approaches give a consistent ordering: Tm_K is the dominant feature by a wide margin, thickness is second, and data source is third. Growth rate R and pressure P contributes smaller but not ignorable, while crystal structure is consistently secondary. Alloy_type and temperature T appear least influential in this dataset, suggesting either limited variability, correlation with other features, or weaker direct relevance to the target as represented here.

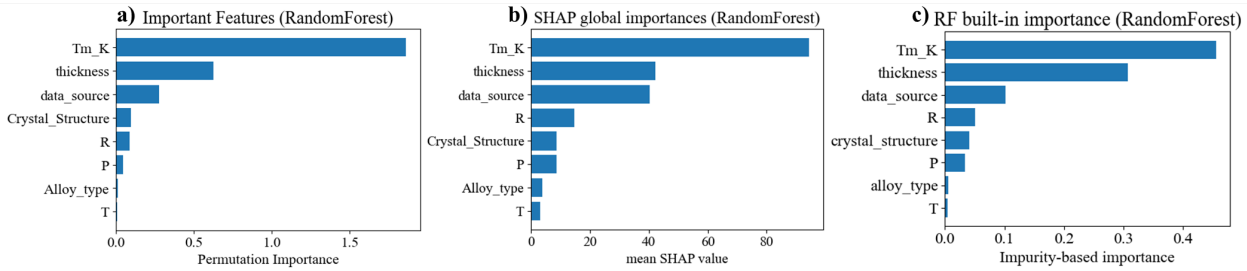

Figure 9, global importance for the data grouping by R for a) sklearn perturbation importance, b) SHAP global importance and c) Random Forest built-in importance

Local interpretation is shown in figure 10 by SHAP for the Random Forest model. Here we show the comparison between data at 5 nm (thickness) and 94 nm for Abermann Ag data. The data at 5 nm witness a much higher negative influence on the thickness and Tm_K. On the contrast, the data at 94 nm is given positive influence from Tm_K and thickness. Both data have positive and same influence on data source, alloy type and R. It validates our model as two data have the same values on these features.

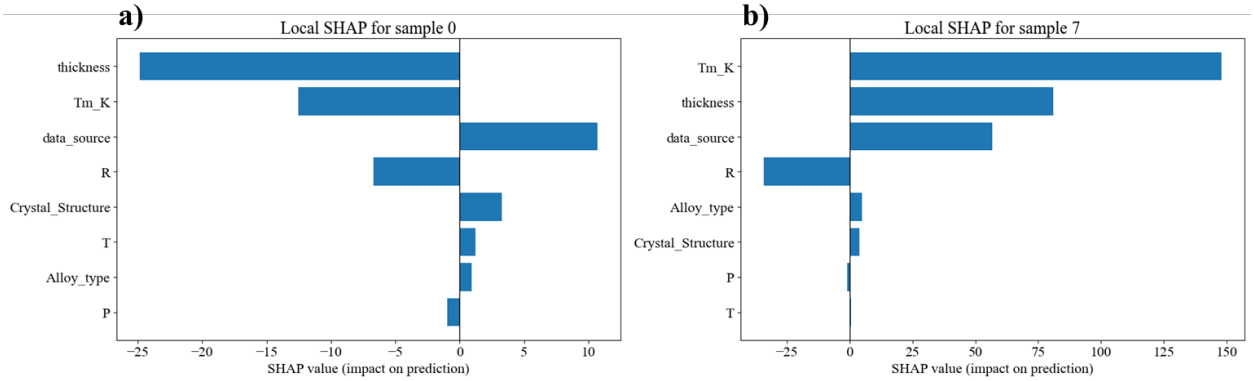

Figure 10, local importance for the data grouping by R for Abermann (data source), Ag, 0.1 nm/s (growth rate), 300 K (temperature) and 0 Pa (pressure) at a) 5 nm and b) 94 nm

5. Outlook

The current model can only confident prediction within certain experiments groups and predict the unknown process conditions (R). From the suggestion of the importance matrix, the next step would be to add more physical constraint to the model to help it learn the relationship between stress-thickness and processing conditions. For example, the energetic impacts (which describe the Vegard's law on the solid solution) can give better explanations on how the high atoms create compressive stress in the thin film.

The model only uses metallic data in the thin film stress dataset while the intermetallic thin films also have high value on the coating for energy, electrode and mechanical films. Therefore, if the ML model on the metallic film stress can be stabilized, we should extend the model to cover other kinds of the alloy system.

Steady state stress is another very important representation in thin film stress. When the thickness of film gets larger (mostly higher than 200 nm), the slope of the stress-thickness curve becomes constant, and this slope is called steady state stress. Using steady state stress, we can analyze and predict the stress evolution in thicker films without knowing the exact deposition thickness. Figure 11 shows the steady state stress vs growth rate for V-W binary solid solution systems. In short, by adding more W content to the solution we can make stress more compressive and behave more like pure W. It would be another great direction to improve the ML model.

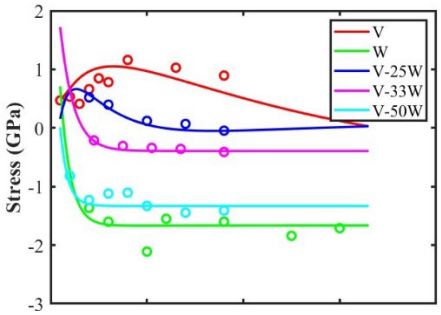

Figure 11, the steady state stress for V-W binary solid solution

Furthermore, we can add uncertainty estimation to the model. As figure 12 shows, we can have the respective uncertainty/error on each parameter and get the uncertainty bands on the predictions. It can give better interpretation of our stress-thickness predictions: instead of just an absolute solution, we can give the upper and lower bands with certain criteria (75% or 95% confidence). It will be better instruction for the experimental tunning as we can have a stress range and more room for the improvement on processing conditions.

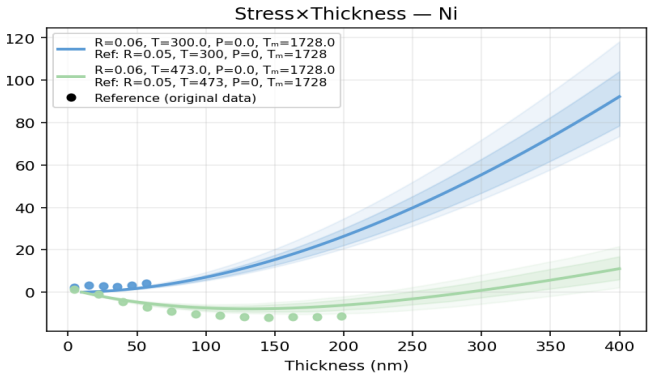

Figure 12, the prediction on unknown conditions (growth rate) for Ni with uncertainty bands.

Reference

[1] P. Waters, A.A. Volinsky, Stress and moisture effects on thin film buckling delamination, Exp. Mech. 47(1) (2007) 163-170.
[2] J. Matovic, Application of Ni electroplating techniques towards stress-free microelectromechanical system-based sensors and actuators, Proc. Inst. Mech. Eng. C: J. Mech. Eng. Sci. 220(11) (2006) 1645-1654.
[3] D. Vogel, E. Auerswald, J. Auersperg, P. Bayat, R.D. Rodriguez, D.R.T. Zahn, S. Rzepka, B. Michel, Stress analyses of high spatial resolution on TSV and BEoL structures, Microelectron. Reliab. 54(9-10) (2014) 1963-1968.
[4] R. Koch, The Intrinsic Stress of Polycrystalline and Epitaxial Thin Metal-Films, J. Phys.: Condens. Matter 6(45) (1994) 9519-9550.
[5] E. Chason, P.R. Guduru, Tutorial: Understanding residual stress in polycrystalline thin films through real-time measurements and physical models, J. Appl. Phys. 119(19) (2016) 191101.
[6] G. Abadias, E. Chason, J. Keckes, M. Sebastiani, G.B. Thompson, E. Barthel, G.L. Doll, C.E. Murray, C.H. Stoessel, L. Martinu, Review Article: Stress in thin films and coatings: Current status, challenges, and prospects, J. Vac. Sci. Technol. A 36(2) (2018) 020801.
[7] E. Chason, T. Su, Understanding the Origins of Residual Stress in Thin Films Through Measurements and Modeling, Jom-Us (2025).
[8] E. Chason, J.W. Shin, S.J. Hearne, L.B. Freund, Kinetic model for dependence of thin film stress on growth rate, temperature, and microstructure, J. Appl. Phys. 111(8) (2012) 083520
[9] R. Koch, D. Winau, A. Fuhrmann, K.H. Rieder, Growth-Mode-Specific Intrinsic Stress of Thin Silver Films, Phys Rev B 44(7) (1991) 3369-3372.
[10] R. Abermann, R. Koch, Internal-Stress of Thin Silver and Gold-Films and Its Dependence on Gas-Adsorption, Thin Solid Films 62(2) (1979) 195-208.
[11] R. Abermann, R. Koch, Insitu Study of Thin-Film Growth by Internal-Stress Measurement under Ultrahigh-Vacuum Conditions - Silver and Copper under the Influence of Oxygen, Thin Solid Films 142(1) (1986) 65-76.
[12] D. Flötotto, Z.M. Wang, L.P.H. Jeurgens, E. Bischoff, E.J. Mittemeijer, Effect of adatom surface diffusivity on microstructure and intrinsic stress evolutions during Ag film growth, J Appl Phys 112(4) (2012).
[13] A.L. Shull, F. Spaepen, Measurements of stress during vapor deposition of copper and silver thin films and multilayers, J. Appl. Phys. 80(11) (1996) 6243-6256.
[14] S.C. Seel, C.V. Thompson, S.J. Hearne, J.A. Floro, Tensile stress evolution during deposition of Volmer–Weber thin films, J. Appl. Phys. 88(12) (2000) 7079–7088
[15] T. Kaub, R. Anthony, G.B. Thompson, Intrinsic stress response of low and high mobility solute additions to Cu thin films, J. Appl. Phys. 122(22) (2017).
[16] M. Pletea, W. Brückner, H. Wendrock, R. Kaltofen, R. Koch, In situ stress evolution of Co films sputtered onto oxidized Si (100) substrates, J. Appl. Phys. 99(3) (2006) 033509.
[17] G. Thurner, R. Abermann, Internal-Stress and Structure of Ultrahigh-Vacuum Evaporated Chromium and Iron Films and Their Dependence on Substrate-Temperature and Oxygen Partial-Pressure during Deposition, Thin Solid Films 192(2) (1990) 277-285.
[18] E. Klokholm, B.S. Berry, Intrinsic Stress in Evaporated Metal Films, J. Electrochem. Soc. 115(8) (1968) 823-&.
[19] D.W. Hoffman, J.A. Thornton, Internal-Stresses in Sputtered Chromium, Thin Solid Films 40(Jan) (1977) 355-363.

[20] X.Y. Zhou, T. Kaub, R.L. Martens, G.B. Thompson, Influence of Fe(Cr) miscibility on thin film grain size and stress, Thin Solid Films 612 (2016) 29-35.
[21] X.Y. Zhou, G.B. Thompson, The influence of alloying interactions on thin film growth stresses, Appl. Surf. Sci. 463 (2019) 545-555.
[22] D. Chocyk, T. Zientarski, A. Proszynski, T. Pienkos, L. Gladyszewski, G. Gladyszewski, Evolution of stress and structure in Cu thin films, Cryst. Res. Technol. 40(4-5) (2005) 509-516.
[23] C. Friesen, C.V. Thompson, Correlation of stress and atomic-scale surface roughness evolution during intermittent homoepitaxial growth of (111)-oriented Ag and Cu - art. no. 056104, Phys Rev Lett 93(5) (2004).
[24] D. Winau, R. Koch, A. Fuhrmann, K.H. Rieder, Film Growth-Studies with Intrinsic Stress Measurement - Polycrystalline and Epitaxial Ag, Cu, and Au Films on Mica(001), J Appl Phys 70(6) (1991) 3081-3087.
[25] M. Pletea, W. Brückner, H. Wendrock, R. Kaltofen, Stress evolution during and after sputter deposition of Cu thin films onto Si (100) substrates under various sputtering pressures, J. Appl. Phys. 97(5) (2005) 054908.
[26] T. Kaub, Z.X. Rao, E. Chason, G.B. Thompson, The influence of deposition parameters on the stress evolution of sputter deposited copper, Surf. Coat. Technol. 357 (2019) 939-946.
[27] T.M. Kaub, P. Felfer, J.M. Cairney, G.B. Thompson, Influence of Ni Solute segregation on the intrinsic growth stresses in Cu(Ni) thin films, Scripta Mater 113 (2016) 131-134.
[28] D. Winau, R. Koch, K.H. Rieder, The Influence of Oxygen on Intrinsic Stress and Growth of Iron and Nickel Films, Applied Physics Letters 59(9) (1991) 1072-1074.
[29] B. Fu, G.B. Thompson, Compositional dependent thin film stress states, J. Appl. Phys. 108(4) (2010).
[30] X.Y. Zhou, G.B. Thompson, Influence of solute partitioning on the microstructure and growth stresses in nanocrystalline Fe(Cr) thin films, Thin Solid Films 648 (2018) 83-93.
[31] A. Fillon, G. Abadias, A. Michel, C. Jaouen, Stress and microstructure evolution during growth of magnetron-sputtered low-mobility metal films: Influence of the nucleation conditions, Thin Solid Films 519(5) (2010) 1655-1661.
[32] H.Z. Yu, C.V. Thompson, Grain growth and complex stress evolution during Volmer–Weber growth of polycrystalline thin films, Acta Mater. 67 (2014) 189-198.
[33] T.R. Koenig, Z.X. Rao, E. Chason, G.J. Tucker, G.B. Thompson, The microstructural and stress evolution in sputter deposited Ni thin films, Surf. Coat. Technol. 412 (2021).
[34] G. Lumbeeck, A. Delvaux, H. Idrissi, J. Proost, D. Schryvers, Analysis of internal stress build-up during deposition of nanocrystalline Ni thin films using transmission electron microscopy, Thin Solid Films 707 (2020).
[35] H.J. Schneeweiss, R. Abermann, Ultra-High Vacuum Measurements of the Internal-Stress of Pvd Titanium Films as a Function of Thickness and Its Dependence on Substrate-Temperature, Vacuum 43(5-7) (1992) 463-465.
[36] J.A. Floro, S.J. Hearne, J.A. Hunter, P. Kotula, E. Chason, S.C. Seel, C.V. Thompson, The dynamic competition between stress generation and relaxation mechanisms during coalescence of Volmer-Weber thin films, J. Appl. Phys. 89(9) (2001) 4886-4897.
[37] H.J. Schneeweiss, R. Abermann, On the Influence of the Substrate Properties on the Internal Growth Stress of Titanium Films at 250-Degrees-C, Thin Solid Films 228(1-2) (1993) 40-43.
[38] T. Kaub, G.B. Thompson, Ti segregation in regulating the stress and microstructure evolution in W-Ti nanocrystalline films, J. Appl. Phys. 122(8) (2017).

[39] T. Su, J. Robinson, G.B. Thompson, E. Chason, Stress evolution in sputtered vanadium-tungsten alloys, Surf. Coat. Technol. 475 (2023).
[40] J.A. Johnson, T. Su, E. Chason, G.B. Thompson, Inter-relationship of stress and microstructure in BCC and 'beta' tungsten films, Surf. Coat. Technol. 457 (2023).